

Water-Dispersible Oil-Filled ABC Triblock Copolymer Vesicles and Nanocapsules

Ronghua Zheng and Guojun Liu*

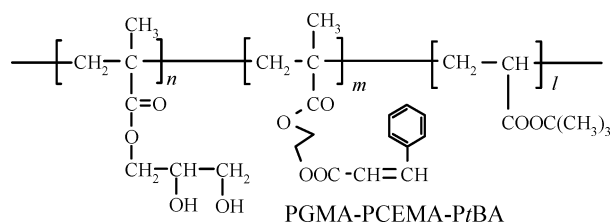
Department of Chemistry, Queen's University, 90 Bader Lane, Kingston, Ontario, Canada K7L 3N6

Received January 25, 2007; Revised Manuscript Received April 25, 2007

ABSTRACT: Customer-engineered block copolymers can self-assemble under appropriate conditions in block-selective solvents into vesicles. Such vesicles have been of enormous academic interest over the past decade for their potential applications in enzyme encapsulation as well as in controlled release of drugs, fragrance, fertilizer, etc. A drawback with the self-assembled vesicles is that the solvent external to and in the internal cavity of a vesicle is essentially the same. This makes loading of reagents into the vesicle cavities difficult. Reported in this paper is a methodology for the one-pot synthesis of water-dispersible oil-filled ABC triblock copolymer vesicles or nanocapsules. Such a methodology achieves reagent (oil) filling and vesicle preparation simultaneously and should help commercial acceptance of block copolymer vesicles.

I. Introduction

Block copolymer self-assembly in block-selective solvent enables the preparation of nanoaggregates with shape^{1,2} ranging from spheres³ to cylinders,^{1–4} vesicles,^{5–11} donuts,^{12–14} and many more.¹⁵ Of the various aggregates, vesicles have attracted much attention for their potential applications^{16–22} in controlled release of drugs, pheromone, fragrance, and fertilizers, in enzyme encapsulation, in template synthesis, in catalysis, and in other areas. Vesicles prepared by block copolymer self-assembly possess normally the same solvent or solvent mixture in their cavity and dispersing medium, and the loading of reagents into the vesicle cavities is not straightforward.^{16,19,23} In this paper, we report a strategy that accomplishes vesicle preparation and reagent or oil loading simultaneously and thus overcomes the reagent-loading difficulty. This is done via an oil-in-water emulsion process using decahydronaphthalene (DN) as the model loading agent or oil and poly(glyceryl methacrylate)-*block*-poly(2-cinnamoyloxyethyl methacrylate)-*block*-poly(*tert*-butyl acrylate) or PGMA–PCEMA–PtBA as the surfactant, where the PGMA block is water-soluble, the PCEMA block is soluble in neither oil nor water and is photo-cross-linkable, and the PtBA block is oil-soluble. Such vesicles can be further cross-linked to yield “permanent” vesicles or nanocapsules.



While block copolymers have long been used as surfactants to stabilize oil and sometimes monomer droplets in water or water droplets in oil,^{24–30} we believe that our method for preparation of cross-linked block copolymer nanocapsules filled with oil is novel. The vesicles prepared from this approach before PCEMA cross-linking resemble very much a self-assembled ABC triblock vesicle as reported by Eisenberg and co-workers,³¹ Lecommandoux and co-workers,⁷ and Schlaad and

co-workers.³² Our nanocapsules also bear structural resemblance to cross-linked block copolymer vesicles prepared from AB diblocks^{17,23,33–35} or hollow nanospheres derived from ABC block copolymer micelles that have undergone selective B block cross-linking and C block degradation.^{36,37}

Aside from use of block copolymers, there are many other methods for encapsulation.^{18,38,39} Traditionally, encapsulation is achieved mainly via interfacial polymerization,^{40–43} which yields capsules with sizes mostly in the micrometer range.^{20,21} When combined with miniemulsion formation, submicrometer capsules can also be prepared.⁴⁴ More recently, there have been reports on preparation of nanocapsules based on cross-linking of ligands attached to quantum dots^{45,46} or monomers embedding polymer microspheres⁴¹ at water/oil interfaces. There have also been reports on oil droplet production and then interfacial polymerization in microfluidic devices.^{47,48} Then, one can prepare nanocapsules by controlled emulsion, miniemulsion, or suspension polymerization in which the monomer or monomers polymerize preferentially at the oil and water interface and precipitate out there.^{39,49,50} Alternatively, one can prepare nanocapsules by cross-linking liposomes preformed from small-molecule surfactants.^{18,51–53} Polymer nanocapsules can be prepared also starting from a solid template that includes metal nanoparticles, silica nanoparticles, or polymer nanoparticles. Nanocapsules are obtained by dissolving the template after polymer has been deposited onto the template by the layer-by-layer protocol⁵⁴ or by direct polymerization.^{55,56}

II. Experimental Section

Materials and Reagents. PGMA–PCEMA–PtBA was synthesized following procedures described previously.⁵⁷ Methanol (99.8%, Fisher), methylene chloride (95.5%, Fisher), trifluoroacetic acid (99%, Aldrich), DN (mixture of *cis* and *trans*, 98%, Aldrich), deuterated solvents methanol (CD₃OD, 99.8%, Cambridge Isotope Laboratories or CIL), deuterated methylene chloride (CD₂Cl₂, 99.9%, Aldrich), deuterium oxide (D₂O, 99.9%, CIL), and deuterated DN (C₁₀D₁₈, mixture of *cis* and *trans*, 99%, CIL) were all used as received.

Nanocapsule Preparation via the Ideal Scheme. All preparations were carried out in a 100 mL three-neck round-bottom flask immersed in an oil bath. To one end of the stirring shaft of a mechanical stirrer was mounted a hemispherically shaped Teflon blade, which was 4.8 cm wide and 2.0 cm tall. The blade was

* Corresponding author. E-mail: guojun.liu@chem.queensu.ca.

inserted into the flask via the middle joint of the flask. Water (38 mL) and DN/MC at $v/v = 1/1$ were added into the flask. Under stirring at 1500 or 800 rpm was added dropwise 0.40 mL of MC/methanol at $v/v = 1/1$ containing 10 mg of PGMA–PCEMA–PtBA. After stirring at room temperature for 30 min, the system was heated at 35 °C for 2 h and at 50 °C for 1 h. To cross-link the PCEMA layer, the emulsion was irradiated in the round-bottom flask under magnetic stirring at 20 °C for ~20 h by UV light from a Universal lamp power supply system equipped with a 500 W Hg lamp. To determine PCEMA double conversion, the sample was diluted 10 times with water and the absorbance decrease at 274 nm was monitored.⁵⁸ Typical PCEMA double conversion used was 40%.

Nanocapsule Preparation Using DN Alone as the Oil Phase.

The apparatus used, the apparatus setup protocol, and the amount of water used were the same as described above. Instead of using a mixture of DN and MC as the oil phase, 0.33 mL of DN was used alone as the oil phase. After the mixing of 38 mL of water and 0.33 mL of DN, the mixture was heated to 90 °C. Under mechanical stirring at 1500 rpm, 0.40 mL of MC/methanol at $v/v = 1/1$ containing 10 mg of PGMA–PCEMA–PtBA was added dropwise. This mixture was stirred at this temperature for 3 h before it was cooled and irradiated under magnetic stirring with UV at 20 °C for 17 h.

Nanocapsule Characterization. Before routine TEM check nanocapsules in water after preparation were aspirated on to nitrocellulose-coated copper grids and stained by OsO₄ for 2 h. To locate the PtBA chains by TEM, a sample was dialyzed against methanol to achieve solvent switching. Methanol was then removed by rota-evaporation, and ~5 mg of the nanocapsules was redispersed in 1.5 mL of MC. To the dispersion was then added 0.5 mL of trifluoroacetic acid. The mixture was stirred at room temperature for 3 h to hydrolyze PtBA to poly(acrylic acid), PAA, before it was added into diethyl ether to precipitate the capsules. After stirring with 5 mL of water for 1 day, the sample was aspirated on to a nitro-cellulose-coated copper grid. A drop of uranyl acetate at 1 wt % in water/ethanol ($v/v = 9/1$) was added onto the grid to stain the PAA chains for 30 min. This drop was subsequently removed by filter paper, and the stained capsules were rinsed with water droplets eight times.

For DLS characterization, the nanocapsule aqueous solutions were clarified by filtration through 1.2 μm glass microfiber membrane filters (Fisher). DLS measurements were carried out at 45°, 60°, 75°, and 90°, and the data at each angle were analyzed by the cumulant method⁵⁹ to obtain the hydrodynamic diameter d_h and polydispersity K_2^2/K_4 for the capsules.

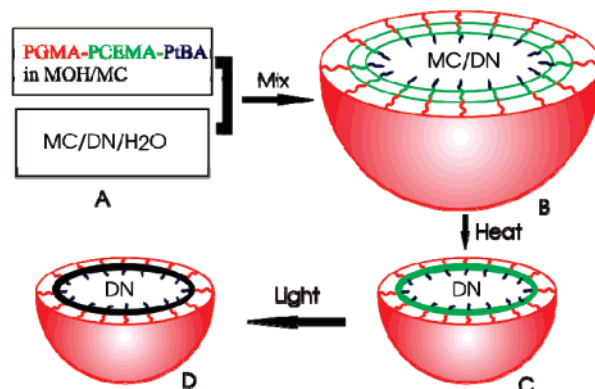
Tapping-mode atomic force microscopy (AFM) analysis was carried out on a Veeco multimode instrument equipped with a Nanoscope IIIa controller. The tips used were of the super sharp Nanosensors SSS-NCHR-SPL type. The images were obtained using a free tip oscillation amplitude A_0 of 60 nm and a set point amplitude ratio R_{sp} of ~90%. The substrate used was of prime grade silicon wafer with orientation (100) purchased from Silicon Quest International.

Nanocapsule Formation Mechanism Probe by ¹H NMR. Mixed in a 25 mL round-bottom flask were 0.60 mL of DN-*d*₁₈/MC-*d*₂ at $v/v = 1/1$ and 4.0 mL of D₂O. CD₃OD/MC-*d*₂ at $v/v = 1/1$, 0.40 mL containing 15 mg of dissolved PGMA–PCEMA–PtBA, was then added into the mixture under magnetic stirring at 1150 rpm. After stirring for 30 min at room temperature, a sample at ~0.8 mL was taken for NMR analysis. The rest was heated at 35 °C for 2 h and at 50 °C for 1 h. After cooling, another sample at ~0.8 mL was taken for NMR analysis. The residual mixture was photolyzed to achieve a PCEMA conversion of 55%. This was followed by rota-evaporation of D₂O to a final volume of ~0.1 mL. To the concentrated sample under stirring was added 3 mL of CDCl₃ to aggregate the nanocapsules. After stirring the mixture for 3 h, the mixture was left standing and the bottom liquid phase was decanted. The CDCl₃ addition, stirring, and removal procedure was repeated, and the residual CDCl₃ was removed by blowing N₂

Table 1. Properties of the PGMA–PCEMA–PtBA Triblock Used Characterized in the PSMA–PCEMA–PtBA Form

SEC M_w/M_n	dn_r/dc (mL/g)	LS $M_w \times 10^{-4}$ (g/mol)	NMR $n/m/l$	n_w	m_w	l_w
1.15	0.108	12.2	3.3/1.59/1.00	335	160	100

Scheme 1. Ideal Scheme for the Preparation of Water-Dispersible DN-Filled PGMA–PCEMA–PtBA Nanocapsules



for 2 min on the solid residual. After redispersion in D₂O for 12 h, the sample was analyzed by NMR.

III. Results and Discussion

Polymer Synthesis and Characterization. The precursor to PGMA–PCEMA–PtBA was synthesized by anionic polymerization. Since the methodology has been described before,⁵⁷ it was not repeated in the Experimental Section or here. For solubility reasons, the polymer was characterized in the PSMA–PCEMA–PtBA form, where PSMA denotes poly(solketal methacrylate). The size exclusion chromatography (SEC) polydispersity index M_w/M_n was measured in DMF based on PS standards. The specific refractive index increment dn_r/dc and light scattering (LS) weight-average molar mass M_w were determined in THF. The ratios $n/m/l$ between the numbers of repeat units for the PSMA, PCEMA, and PtBA blocks were determined from ¹H NMR analysis. Table 1 summarizes the characteristics of the samples used in this study, where n_w , m_w , l_w denote the weight-average numbers of repeat units for the PSMA, PCEMA, and PtBA blocks, respectively.

Nanocapsule Preparation. Nanocapsule preparation started with dissolution of PGMA–PCEMA–PtBA in a small amount of methylene chloride (MC) and methanol and the mixing of water and oil, where the oil can be either DN alone or DN and MC at $v/v = 1/1$. Under vigorous stirring, the triblock solution was then added into the water/oil mixture (A → B, Scheme 1). In the ideal scheme involving DN/MC as the oil phase, MC was evaporated from the oil droplets stabilized by the triblock by raising temperature, which was accompanied by PCEMA chain collapsing (B → C). Nanocapsules with entrapped DN were produced after PCEMA photo-cross-linking (C → D).

Although either DN alone or a binary DN/MC mixture could be used as oil phase, we preferred to start with a binary mixture because we thought that better defined nanocapsules could be obtained if the PCEMA and PtBA blocks were both solubilized initially in the oil phase. This would give the triblock chains translational mobility to smooth out uneven features that might form immediately after their adsorption at the oil/water interface. After some optimization of this ideal scheme, we found that the use of 10 mg of the triblock could disperse 330 μL or less DN in water, and the oil-filled nanocapsules prepared remained stable and dispersed in water for a long time. We achieved our

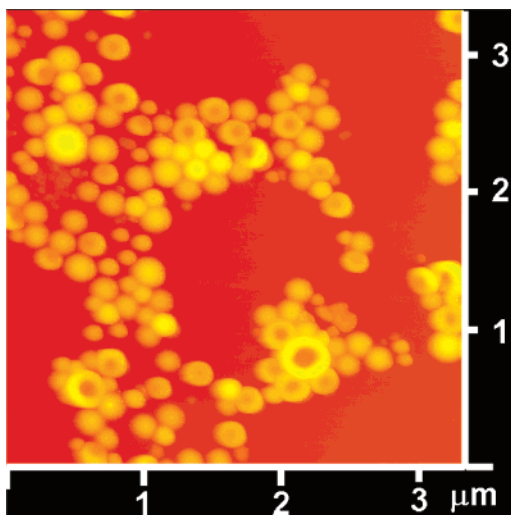


Figure 1. AFM topography image of nanocapsules.

first successful preparation 1 year ago. This sample has been left standing still ever since, and the capsules remain uniformly dispersed up to now.

AFM Characterization of the Capsules. Figure 1 shows an AFM image of nanocapsules thus prepared. The AFM images obtained under ambient conditions show that the particles can be roughly classified into spherical, “donutlike”, and “bowl-shaped” particles.

The spherical particles have a wide range of sizes. The smaller ones might be the regular or swollen core–shell–corona triblock micelles. The larger ones, e.g., those with diameter larger than ~ 150 nm, have to be oil-filled nanocapsules because a fully stretched PGMA–PCEMA–PtBA chain is only ~ 150 nm long. Furthermore, the regular micelles typically have a very narrow size distribution unlike the particles seen here.

Insight into the structural details of the “donutlike” and “bowl-shaped” particles is obtained by examining Figure 2, which provides a 3-d AFM image of several particles and the cross-sectional height analysis result along the green line for two spherical and two “donutlike” particles. Even at the lowest points of the craters in the two seemingly “donutlike” structures, the AFM height readings relative to silicon wafer substrate are not zero but 60 and 58 nm, respectively. The heights for the craters in the other two donutlike particles at points marked by green arrows in the image are 43 and 52 nm, respectively. Since this image was obtained with a super sharp tip which had a width of 10 nm at 120 nm from its even sharper tip front and the craters had diameters ~ 70 nm, the crater depth readings between 15 and 40 nm relative to their ridges have to be real and are not false readings resulting from the tip fatness. The fact that the craters did not have heights close to zero but vastly different height readings suggests they were not donuts but partially collapsed capsules. The crater depth varied because the extent of DN leakage or evaporation varied among the particles. The fact that these structures were not donuts can be appreciated also from the observation that the craters did not lie at the exact center of the particles and the ridges on different sides of a crater had different heights and thicknesses. On the basis of these observations, we believe that the “bowl-shaped” structures in Figure 1 are also partially collapsed nanocapsules with their craters facing sideways.

TEM Characterization of the Capsules. After the aspiration onto a carbon-coated copper grid and the staining of the residual PCEMA double bonds by OsO_4 , we obtained a TEM image of the nanocapsules as shown in the left panel of Figure 3. Aside

from circles with lighter centers (four marked by blue arrows), we see also 2-d projections of what seem to be “bowl-shaped” objects (four marked by green arrows) and many spherical particles with crumpled surfaces (four marked by red arrows).

A circle with a lighter core can be indicative of a spherical PGMA–PCEMA–PtBA micelle, where the lighter core and dark ring correspond to the nonstainable PtBA and the stained PCEMA, respectively, and PGMA is invisible. Circles with light centers can also be projections of nanocapsules,⁶⁰ where the light centers correspond to the PtBA-lined capsule cavities. The four particles marked by blue arrows in the left panel of Figure 3 have an average core–ring diameter of 103 ± 12 nm, which is substantially larger than the length of ~ 65 nm for the fully stretched PCEMA and PtBA chains. Thus, these four particles have to be DN-filled nanocapsules.

The bowl-shaped objects have been seen by AFM and are partially collapsed capsules. Spherical objects with crumpled surfaces were not seen by AFM and must be capsules that have undergone implosion after DN evaporation. Such structures were not seen by AFM but by TEM because AFM was done under ambient conditions, and TEM was performed under high vacuum where DN must have evaporated.

We obtained also TEM images of the capsules after the PtBA chains were hydrolyzed, and the resultant PAA chains were stained by uranyl acetate. Shown in the right panel of Figure 3 is a TEM image of such a sample. Again both bowl-shaped (two marked by green arrows) and wrinkled or crumpled nanocapsules (two marked by red arrows) are seen. We also see capsules, like the two marked by blue arrows, that do not seem to have deformed substantially. In these cases one sees clearly a gray layer external to the dark ring, suggesting the location of PAA or its precursor PtBA on the inner surface of the nanocapsules. The thickness of the dark ring is nonuniform along its circumference probably again because of the nonuniform partial collapse of the nanocapsules along their peripheries. We believe that the thinnest sections of a ring would give the most reasonable estimate for the PAA layer thickness. From the two particles that are marked by blue arrows we determined a thickness of 5 ± 2 nm for the PAA layer, which is comparable to the root-mean-square end-to-end distance of PAA chains with 100 repeat units.

NMR Probing of Capsule Formation Mechanism. Scheme 1 depicts our hypothesized nanocapsule formation mechanism. To verify this, we prepared nanocapsules in deuterated solvents DN- d_{18} , CD_2Cl_2 , CD_3OD , and D_2O and used ^1H NMR to follow the capsule formation process. Figure 4 compares ^1H NMR spectra of samples taken at different stages of nanocapsule formation.

Immediately after mixing PGMA–PCEMA–PtBA with DN- d_{18} , CD_2Cl_2 , and D_2O , we see signals from PGMA between 3.4 and 4.6 ppm and PCEMA between 6.3 and 7.9 ppm. This suggests that both PGMA and PCEMA were in the solvated state. Since PCEMA is only oil-soluble and PGMA is only water-soluble, the two blocks had to be in the separate phases, respectively. The characteristic PtBA peak at 1.5 ppm is unfortunately not resolved for the overwhelming peaks of the undeuterated DN impurities. Since PtBA is soluble in DN/MC and not in water, it has to adopt conformations similar to what is depicted in B of Scheme 1. After CD_2Cl_2 evaporation, the PCEMA peaks between 6.3 and 7.9 ppm disappeared, confirming the segregation of the PCEMA block from the solvent phase as depicted in C of Scheme 1. The formation of a melt-like PCEMA phase greatly reduced the mobility of the PCEMA chains and thus led to the excessive broadening of the PCEMA

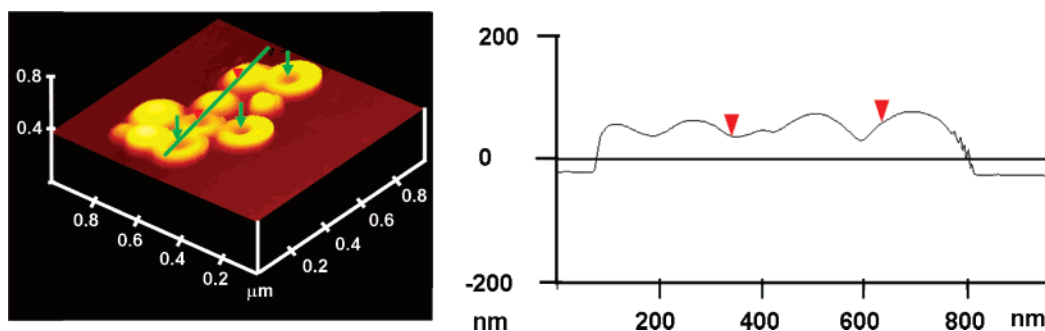


Figure 2. Left: 3-d AFM image of several capsules. Right: height variation along the green line in the left image as a function of distance.

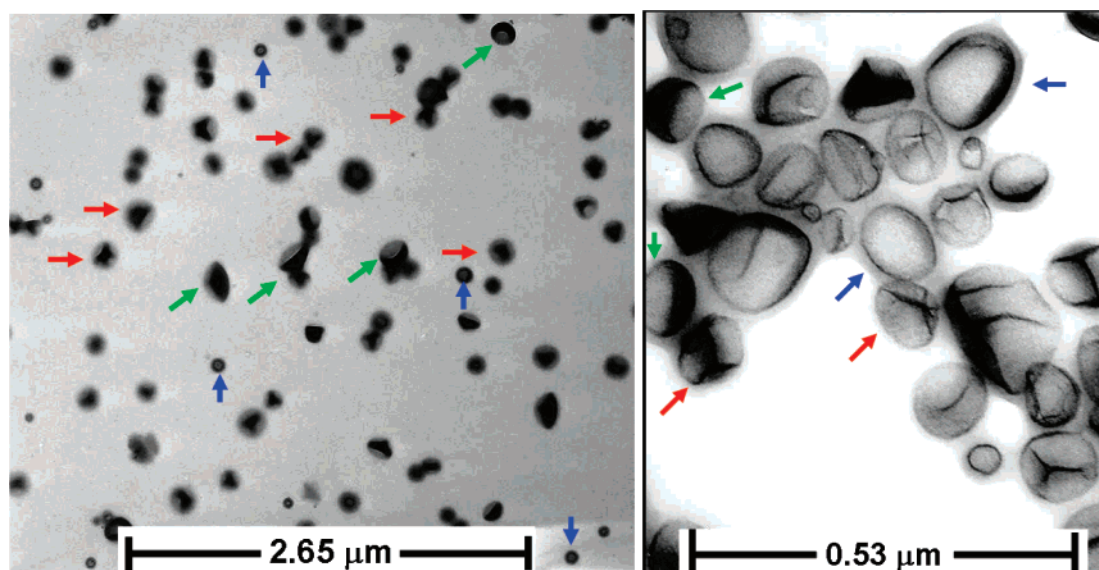


Figure 3. TEM images of nanocapsules. Left: the sample was sprayed from water and stained by OsO_4 . Right: the image was obtained after hydrolyzing PtBA to PAA and staining the sample with $\text{UO}_2(\text{Ac})_2$.

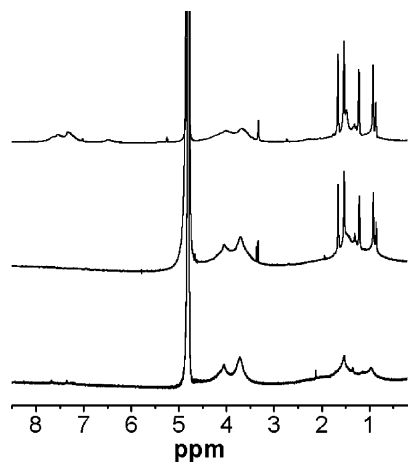


Figure 4. Comparison of ^1H NMR spectra of PGMA-PCEMA-PtBA at different stages of nanocapsule preparation. From top to middle and bottom the spectra were taken respectively after DN- $d_{18}/\text{CD}_2\text{Cl}_2$ droplet formation, after CD_2Cl_2 evaporation, and after PCEMA cross-linking and DN- d_{18} extraction by CDCl_3 .

signals and their disappearance. To eliminate the interference of hydrogenated DN and resolve the PtBA proton peaks, we started by photo-cross-linking the PCEMA layer. Such nanocapsules were then extracted with CDCl_3 to replace DN- d_{18} and its hydrogenated impurities. Shown at the bottom in Figure 4 is a ^1H NMR spectrum of such a sample. The PtBA peak at 1.5 ppm is now clearly visible. Since PtBA is not soluble in water, the observation of its proton peak at 1.5 ppm demonstrates unambiguously that PtBA stretched into the CDCl_3 phase in

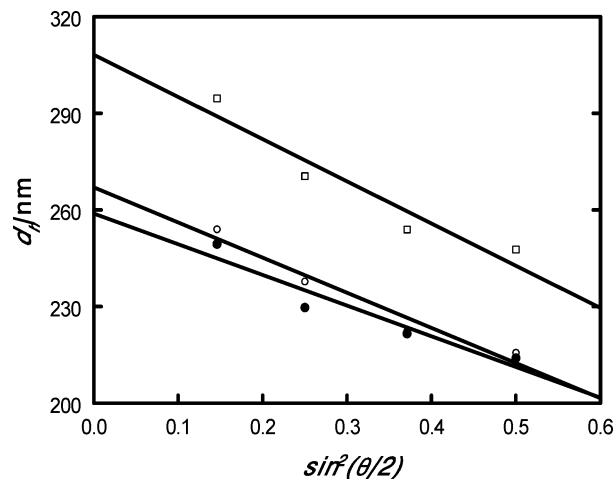


Figure 5. Plot of DLS hydrodynamic diameter d_h vs $\sin^2(\theta/2)$ for PGMA-PCEMA-PtBA vesicles and nanocapsules at different stages: (□) immediately after DN/MC droplet formation, (○) after MC evaporation, and (●) after PCEMA cross-linking.

this case or into the DN phase in the original nanocapsule sample, as depicted in D of Scheme 1.

It should be mentioned that the recipes and experimental protocols used in the preparations involving deuterated and hydrogenated solvents were somewhat different to save costs and to ensure NMR detection of the triblock signals. Despite the recipe and protocol and even possibly end product morphology differences, the solvation states of the different blocks at different stages of nanocapsule production should be the same.

Table 2. Factors Affecting the Size and Size Distribution of the Nanocapsules^a

run	$\nu_{\text{DN}}; \nu_{\text{MC}}$ in mL	stirring speed (rpm)	d_h^0/nm	K_2^2/K_4 at 60°	K_2^2/K_4 at 45°
1	0.33; 0.33	1500	259 ± 9	0.12 ± 0.05	0.11 ± 0.07
2	0.33; 0.33	1500	265 ± 8	0.12 ± 0.05	0.17 ± 0.08
3	0.20; 0.20	1500	266 ± 6	0.15 ± 0.07	0.12 ± 0.07
4	0.33; 0.33	800	275 ± 7	0.13 ± 0.04	0.13 ± 0.04
5 ^b	0.33; 0	1500	216 ± 7	0.20 ± 0.04	0.22 ± 0.03

^a All runs involved the use of 38 mL of water and 10 mg of PGMA–PCEMA–PtBA dissolved in 0.40 mL of $\text{CH}_2\text{Cl}_2/\text{CH}_3\text{OH}$ at $v/v = 1/1$. ^b This run is totally different from the others in preparation protocols.

DLS Probing of Capsule Formation Mechanism. In one nanocapsule preparation we took samples at stages B, C, and D of Scheme 1 for DLS analysis. Figure 5 plots hydrodynamic diameter d_h of the nanocapsules at different stages as a function of $\sin^2(\theta/2)$. Extrapolating to zero scattering angle, we obtained the d_h^0 values of 308 ± 10, 267 ± 6, and 259 ± 9 nm for the capsules at stages B, C, and D, respectively, where the numbers after the “±” sign denote standard deviations in the extrapolated d_h^0 values calculated from the linear regression analysis.⁶¹

That the d_h^0 value of the nanocapsules is the same within experimental error before and after PCEMA cross-linking is in agreement with what we observed for the sizes of spherical micelles of PS–PCEMA before and after PCEMA cross-linking and suggests that the cross-linking did not perturb the morphology of the capsules.¹ The fact that the d_h^0 value decreased by 41 nm or the hydrodynamic volume of the capsules decreased by 35% after CH_2Cl_2 evaporation is in agreement with our hypothesis that CH_2Cl_2 evaporation did not change the number but decreased mainly the size of the capsules.

Control of Nanocapsule Size. Under otherwise identical conditions with water at 38 mL and PGMA–PCEMA–PtBA at 10 mg dissolved in 0.40 mL of $\text{CH}_2\text{Cl}_2/\text{CH}_3\text{OH}$ at $v/v = 1/1$, we found that the use of 2.0 or 1.0 mL of DN/MC at $v/v = 1/1$ as the oil phase yielded products that contained aggregates discernible by the naked eye. Left standing some of the aggregates underwent further agglomeration to form large loose lumps that floated on the water surface. Perfectly stable and well-dispersed samples were prepared by reducing the DN/MC volume to 0.66 mL. Table 2 compares the characteristics of nanocapsules prepared using DN/MC volume equal to or less than 0.66 mL.

Runs 1 and 2 were performed using identical recipes. As expected the d_h^0 values of the final nanocapsules are the same within experimental error. Run 3 was performed using DN/MC less than that used in runs 1 and 2. Surprisingly, the d_h^0 value remains unchanged. Run 4 was performed to examine the effect of varying the stirring speed. Decreasing the speed from 1500 to 800 rpm did lead to a statistically significant increase in d_h^0 , but the increase was not drastic. We did not decrease the stirring speed further as the use of lower stirring speeds lead to polymer precipitation.

Direct Scheme. As explained before, we followed Scheme 1 for most of our preparations because we believed that it would yield better capsules. Step B → C in Scheme 1 could, however, be skipped by using DN alone as the oil phase. In the direct scheme, we performed the preparation using 0.33 mL of DN alone as the oil phase at 90 °C, which is higher than the glass transition temperature of 69 °C for PCEMA⁶⁴ and was used to render PCEMA chain mobility. The capsules produced this way were again very stable in water. More interestingly, the d_h^0 value of the capsules dropped substantially to 216 ± 7 nm (Table 2). A comparison of DLS polydispersity values K_2^2/K_4 for the nanocapsules at the scattering angles of 45° and 60° for different runs in Table 2 indicates that the capsules prepared at 90 °C

had a larger polydispersity. Our TEM analysis of this sample indicated that some short nanotubes were produced together with the nanocapsules from this approach, which explains thus the higher sample polydispersity observed.

IV. Conclusions

Cross-linked polymer nanocapsules have been prepared from PGMA–PCEMA–PtBA using an oil-in-water emulsion process. When DN/MC was used as the oil phase, we established by ¹H NMR and DLS that the nanocapsule formation mechanism followed what is depicted in Scheme 1. Immediately after emulsion formation, the PGMA chains stretched into the aqueous phase, and the PCEMA and PtBA chains were soluble in the oil phase. Evaporation of CH_2Cl_2 from each oil droplet decreased its size and led to the collapse of the PCEMA block. Cross-linking of the PCEMA layer led to permanent nanocapsules, and the structure of the nanocapsules was established by AFM and TEM. The fact that the PtBA block resided in the core of such nanocapsules was established by both ¹H NMR and TEM experiments. Aside from the idealized protocol involving a MC evaporation step the oil-filled nanocapsules could be prepared also using a simpler protocol involving the use of DN alone rather than DN/MC as the oil phase.

Acknowledgment. NSERC of Canada is gratefully acknowledged for sponsoring this research. We appreciate greatly the assistance of Jiandong Wang in obtaining the AFM images. G.L. thanks the Canada Research Chairs program for a research chair position in materials science.

References and Notes

- (1) Tao, J.; Stewart, S.; Liu, G. J.; Yang, M. L. *Macromolecules* **1997**, *30*, 2738–2745.
- (2) Won, Y. Y.; Davis, H. T.; Bates, F. S. *Science* **1999**, *283*, 960–963.
- (3) Cao, L.; Massey, J. A.; Winnik, M. A.; Manners, I.; Riethmuller, S.; Banhart, F.; Spatz, J. P.; Moller, M. *Adv. Funct. Mater.* **2003**, *13*, 271–276.
- (4) Gohy, J. F.; Lohmeijer, B. G. G.; Alexeev, A.; Wang, X. S.; Manners, I.; Winnik, M. A.; Schubert, U. S. *Chem.—Eur. J.* **2004**, *10*, 4315–4323.
- (5) Discher, D. E.; Eisenberg, A. *Science* **2002**, *297*, 967–973.
- (6) Ding, J. F.; Liu, G. J. *Macromolecules* **1997**, *30*, 655–657.
- (7) Rodriguez-Hernandez, J.; Lecommandoux, S. *J. Am. Chem. Soc.* **2005**, *127*, 2026–2027.
- (8) Kesselman, E.; Talmon, Y.; Bang, J.; Abbas, S.; Li, Z. B.; Lodge, T. P. *Macromolecules* **2005**, *38*, 6779–6781.
- (9) Liu, F. T.; Eisenberg, A. *J. Am. Chem. Soc.* **2003**, *125*, 15059–15064.
- (10) Du, J. Z.; Tang, Y. P.; Lewis, A. L.; Armes, S. P. *J. Am. Chem. Soc.* **2005**, *127*, 17982–17983.
- (11) Jenekhe, S. A.; Chen, X. L. *Science* **1998**, *279*, 1903–1907.
- (12) Pochan, D. J.; Chen, Z. Y.; Cui, H. G.; Hales, K.; Qi, K.; Wooley, K. L. *Science* **2004**, *306*, 94–97.
- (13) Zhu, J. T.; Liao, Y. G.; Jiang, W. *Langmuir* **2004**, *20*, 3809–3812.
- (14) Ding, J. F.; Liu, G. J.; Yang, M. L. *Polymer* **1997**, *38*, 5497–5501.
- (15) Cameron, N. S.; Corbierre, M. K.; Eisenberg, A. *Can. J. Chem.* **1999**, *77*, 1311–1326.
- (16) Vriezema, D. M.; Aragones, M. C.; Elemans, J.; Cornelissen, J.; Rowan, A. E.; Nolte, R. J. M. *Chem. Rev.* **2005**, *105*, 1445–1489.
- (17) Kita-Tokarczyk, K.; Grumelard, J.; Haefele, T.; Meier, W. *Polymer* **2005**, *46*, 3540–3563.
- (18) Walde, P.; Ichikawa, S. *Biomol. Eng.* **2001**, *18*, 143–177.

- (19) Broz, P.; Driamov, S.; Ziegler, J.; Ben-Haim, N.; Marsch, S.; Meier, W.; Hunziker, P. *Nano Lett.* **2006**, *6*, 2349–2353.
- (20) Uludag, H.; De Vos, P.; Tresco, P. A. *Adv. Drug Delivery Rev.* **2000**, *42*, 29–64.
- (21) Chang, T. M. S. *Nat. Rev. Drug Discovery* **2005**, *4*, 221–235.
- (22) Yan, M.; Ge, J.; Liu, Z.; Ouyang, P. K. *J. Am. Chem. Soc.* **2006**, *128*, 11008–11009.
- (23) Ding, J. F.; Liu, G. J. *J. Phys. Chem. B* **1998**, *102*, 6107–6113.
- (24) Napper, D. H. *Polymeric Stabilization of Colloidal Dispersions*; Academic Press: London, 1983.
- (25) Riess, G. *Colloids Surf., A* **1999**, *153*, 99–110.
- (26) Muller, H.; Leube, W.; Tauer, K.; Forster, S.; Antonietti, M. *Macromolecules* **1997**, *30*, 2288–2293.
- (27) Lu, Z. H.; Liu, G. J.; Liu, F. T. *Macromolecules* **2001**, *34*, 8814–8817.
- (28) Lu, Z. H.; Liu, G. J.; Phillips, H.; Hill, J. M.; Chang, J.; Kydd, R. A. *Nano Lett.* **2001**, *1*, 683–687.
- (29) Liu, G. J.; Yang, H. S.; Zhou, J. Y. *Biomacromolecules* **2005**, *6*, 1280–1288.
- (30) Zheng, R. H.; Liu, G. J.; Yan, X. H. *J. Am. Chem. Soc.* **2005**, *127*, 15358–15359.
- (31) Luo, L. B.; Eisenberg, A. *Angew. Chem., Int. Ed.* **2002**, *41*, 1001–1004.
- (32) Schrage, S.; Sigel, R.; Schlaad, H. *Macromolecules* **2003**, *36*, 1417–1420.
- (33) Meier, W.; Hirt, T.; Nardin, C. Amphiphilic Polymeric Vesicles. US6916488, 2005.
- (34) Vriezema, D. M.; Hoogboom, J.; Velonia, K.; Takazawa, K.; Christensen, P. C. M.; Maan, J. C.; Rowan, A. E.; Nolte, R. J. M. *Angew. Chem., Int. Ed.* **2003**, *42*, 772–776.
- (35) Discher, B. M.; Won, Y. Y.; Ege, D. S.; Lee, J. C. M.; Bates, F. S.; Discher, D. E.; Hammer, D. A. *Science* **1999**, *284*, 1143–1146.
- (36) Stewart, S.; Liu, G. J. *Chem. Mater.* **1999**, *11*, 1048–1054.
- (37) Huang, H. Y.; Remsen, E. E.; Kowalewski, T.; Wooley, K. L. *J. Am. Chem. Soc.* **1999**, *121*, 3805–3806.
- (38) Meier, W. *Chem. Soc. Rev.* **2000**, *29*, 295–303.
- (39) Landfester, K. *Annu. Rev. Mater. Res.* **2006**, *36*, 231–279.
- (40) Chu, L. Y.; Park, S. H.; Yamaguchi, T.; Nakao, S. *Langmuir* **2002**, *18*, 1856–1864.
- (41) Croll, L. M.; Stover, H. D. H.; Hitchcock, A. P. *Macromolecules* **2005**, *38*, 2903–2910.
- (42) Shulkin, A.; Stover, H. D. H. *J. Membr. Sci.* **2002**, *209*, 421–432.
- (43) Sengupta, A.; Nielsen, K. K.; Barinsteyn, G.; Li, K.; Banovetz, J. P. Adherent Microcapsules Containing Biological Active Ingredients. US 6080418, 2000.
- (44) Scott, C.; Wu, D.; Ho, C. C.; Co, C. C. *J. Am. Chem. Soc.* **2005**, *127*, 4160–4161.
- (45) Russell, J. T.; Lin, Y.; Boker, A.; Su, L.; Carl, P.; Zettl, H.; He, J. B.; Sill, K.; Tangirala, R.; Emrick, T.; Littrell, K.; Thiagarajan, P.; Cookson, D.; Fery, A.; Wang, Q.; Russell, T. P. *Angew. Chem., Int. Ed.* **2005**, *44*, 2420–2426.
- (46) Lin, Y.; Skaff, H.; Boker, A.; Dinsmore, A. D.; Emrick, T.; Russell, T. P. *J. Am. Chem. Soc.* **2003**, *125*, 12690–12691.
- (47) Quevedo, E.; Steinbacher, J.; McQuade, D. T. *J. Am. Chem. Soc.* **2005**, *127*, 10498–10499.
- (48) Zhang, H.; Tumarkin, E.; Peerani, R.; Nie, Z.; Sullan, R. M. A.; Walker, G. C.; Kumacheva, E. *J. Am. Chem. Soc.* **2006**, *128*, 12205–12210.
- (49) Ali, M. M.; Stover, H. D. H. *Macromolecules* **2003**, *36*, 1793–1801.
- (50) Okubo, M.; Konishi, Y.; Minami, H. *Colloid Polym. Sci.* **1998**, *276*, 638–642.
- (51) Ringsdorf, H.; Schlarb, B.; Venzmer, J. *Angew. Chem., Int. Ed. Engl.* **1988**, *27*, 113–158.
- (52) O'Brien, D. F.; Armitage, B.; Benedicto, A.; Bennett, D. E.; Lamparski, H. G.; Lee, Y. S.; Srisiri, W.; Sisson, T. M. *Acc. Chem. Res.* **1998**, *31*, 861–868.
- (53) Song, L. Y.; Ge, X. W.; Wang, M. Z.; Zhang, Z. C.; Li, S. C. *J. Polym. Sci., Part A: Polym. Chem.* **2006**, *44*, 2533–2541.
- (54) Caruso, F.; Caruso, R. A.; Mohwald, H. *Science* **1998**, *282*, 1111–1114.
- (55) Marinakos, S. M.; Novak, J. P.; Brousseau, L. C.; House, A. B.; Edeki, E. M.; Feldhaus, J. C.; Feldheim, D. L. *J. Am. Chem. Soc.* **1999**, *121*, 8518–8522.
- (56) Kamata, K.; Lu, Y.; Xia, Y. N. *J. Am. Chem. Soc.* **2003**, *125*, 2384–2385.
- (57) Yan, X.; Liu, G.; Li, Z. *J. Am. Chem. Soc.* **2004**, *126*, 10059–66.
- (58) Guo, A.; Liu, G. J.; Tao, J. *Macromolecules* **1996**, *29*, 2487–2493.
- (59) Berne, B. J.; Pecora, R. *Dynamic Light Scattering with Applications to Chemistry, Biology, and Physics*; Dover Publications: Mineola, NY, 1976.
- (60) Zhang, L. F.; Eisenberg, A. *Science* **1995**, *268*, 1728–1731.
- (61) Christian, G. D. *Analytical Chemistry*; John Wiley & Sons: New York, 1994.
- (62) Schork, F. J.; Luo, Y. W.; Smulders, W.; Russum, J. P.; Butte, A.; Fontenot, K. Miniemulsion polymerization. In *Polym. Particles* **2005**, *175*, 129–255.
- (63) Faber, K. *Biotransformations in Organic Chemistry*, 5th ed.; Springer: Berlin, 2004.
- (64) Liu, G. J.; Ding, J. F.; Qiao, L. J.; Guo, A.; Dymov, B. P.; Gleeson, J. T.; Hashimoto, T.; Saijo, K. *Chem.—Eur. J.* **1999**, *5*, 2740–2749.

MA070215U